Controlling the Growth of Si/Ge Nanowires and Heterojunctions Using Silver–Gold Alloy Catalysts

Yi-Chia Chou,[†] Cheng-Yen Wen,[†,∥] Mark C. Reuter,[‡] Dong Su,[§] Eric A. Stach,[†,§,*] and Frances M. Ross[‡,*]

[†]School of Materials Engineering and Birck Nanotechnology Center, Purdue University, West Lafayette, Indiana 47907, United States , [‡]IBM T. J. Watson Research Center, Yorktown Heights, New York 10598, United States , [§]Center for Functional Nanomaterials, Brookhaven National Laboratory, Upton, New York 11973, United States. [∥]Current Address: Department of Materials Science and Engineering, National Taiwan University, Taipei, 106, Taiwan.

ABSTRACT

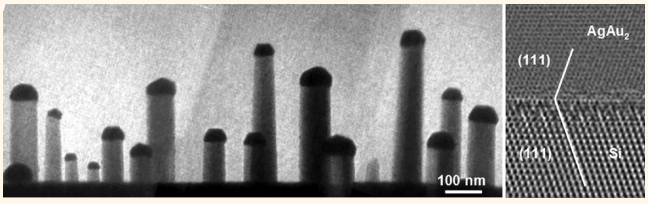

We describe a new catalyst for group IV nanowire heterostructures, based on alloying Ag with Au, that combines the ability to control catalyst phase and nanowire structure with good environmental stability. Compared to other alloy catalysts, we show a higher oxidation resistance of AgAu and more consistent crystal shapes and catalyst/nanowire orientation relationships during growth. We show that AgAu catalysts are also stable against diffusion during growth, making them capable of forming long nanowires with uniform diameters. Furthermore, we demonstrate the growth of compositionally abrupt Si/Ge heterojunctions with good reproducibility and yield, switching individual nanowires between vapor–liquid–solid and vapor-solid–solid growth to optimize growth rates by control of the catalyst state. The stability and properties of AgAu catalysts potentially open up a promising and practical route toward control of group IV heterostructure nanowires.

KEYWORDS: nanowire growth · Si/Ge heterojunctions · AgAu alloys · vapor–solid–solid growth · *in situ* transmission electron microscopy

A range of nanowire applications, including tunnel field effect transistors and thermoelectrics,[1−4] would benefit from the ability to form Si/Ge heterostructure nanowires with compositionally abrupt interfaces. However, the conventional approach to nanowire growth, using the vapor–liquid–solid (VLS) mechanism with catalysts based on Au,[5,6] is fundamentally unable to form abrupt Si/Ge heterojunctions. This is because the liquid catalyst droplet acts as a reservoir when switching between growth materials.[7,8] Heterojunction diffuseness can be reduced to some extent by alloying liquid catalysts[9] or by modulating growth pressure,[10] but atomically abrupt heterojunctions have only been demonstrated using one catalyst, $AlAu_2$. This is solid during growth and thus has a low solubility for the growth species.[11] However, it is air-sensitive which complicates its use for practical nanowire growth.

To develop a simpler route to the control of Si/Ge nanowire heterostructures, we therefore propose the use of silver-based alloy catalysts. The choice of Ag is motivated by several aspects of the phase diagrams of Ag with Si, Ge, and Au. Minimizing the solubility of Si and Ge in the catalyst, as required to reduce the reservoir effect and therefore create abrupt heterojunctions, suggests the need for a solid phase catalyst[7] and thus growth *via* the vapor–solid–solid (VSS) mechanism. The catalyst must be solid at temperatures that are "reasonable" for nanowire growth: low enough to avoid interdiffusion of Si and Ge during growth, yet high enough to achieve a growth rate that is not too slow. Pure Au is unsuitable because VSS growth can only be sustained for Si and Ge at temperatures below its eutectic temperature (~360 °C for both Si and Ge), where the growth rate of Si would be slow.[12] Al, which also forms simple eutectics with Si and Ge,[13] is difficult to use since it oxidizes so readily that both the deposition of the catalyst and the growth of the nanowires must take place under ultrahigh vacuum (UHV) conditions to obtain a good yield of high quality nanowires.[14,15] Like Au and Al, Ag forms eutectics with Si and Ge,[13] but is not as environmentally sensitive as Al. The eutectic temperatures are 850 and 650 °C for Si and Ge, respectively, and growth of Si/Ge heterostructured nanowires with a solid Ag catalyst may thus be expected to take place at temperatures higher than are possible using pure Au.

* Address correspondence to estach@bnl.gov, fmross@us.ibm.com.

Received for review May 4, 2012 and accepted June 18, 2012.

Published online June 18, 2012
10.1021/nn301978x

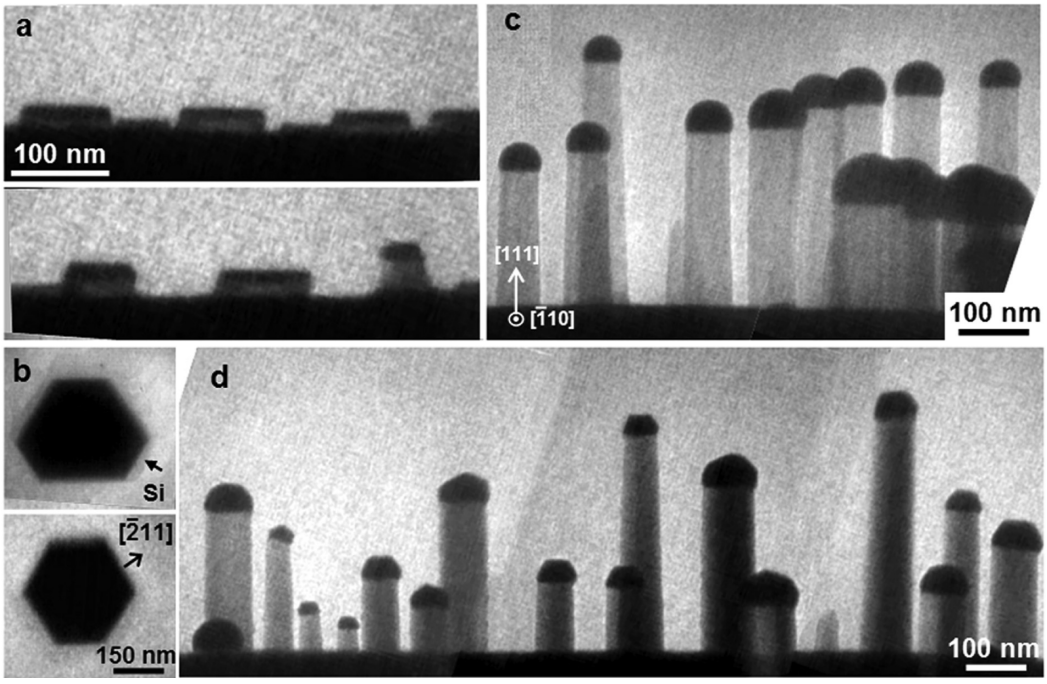

Figure 1. Si nanowire growth in the VLS and VSS modes. (a) Si nanowires imaged during VSS growth from Ag_2Au at 512 °C and 5×10^{-6} Torr disilane. The growth temperature is below both the calculated T_E for Ag_2Au with Si of 710 °C, and the lowest temperature at which liquid is expected to be present on the calculated phase diagram, 610 °C. (b) Plan view images of nanowire growth from Ag_2Au at 530 °C and 1×10^{-5} Torr disilane. The arrow indicates the base of the Si nanowire growing beneath the catalyst. A Si ⟨211⟩ direction is also shown. (c) Longer Si nanowires during VLS growth from $AgAu_2$ at 556 °C and 1×10^{-5} Torr disilane. The growth temperature is above the calculated T_E for $AgAu_2$ of 536 °C. (d) The same sample as in panel c but now showing VSS growth, obtained by cooling to 360 °C in 1×10^{-5} Torr disilane.

Ag has been used to grow crystalline Si nanowires at very high temperatures, ~1000 °C,[16,17] presumably with liquid catalysts. At lower temperatures (below 500 °C), ultrathin defective nanowires have been formed, presumably with solid catalysts.[18] However, as we show with the following, pure Ag catalysts suffer from an instability caused by surface diffusion, limiting their use at higher temperatures. To increase our flexibility in controlling growth, we therefore note that Ag is miscible with Au and does not form intermetallic compounds.[12] This opens up the possibility of tuning growth parameters such as catalyst state (solid *versus* liquid) and growth rate, in a continuous fashion, by alloying Ag with Au. AgAu alloys have pseudobinary phase diagrams with Si or Ge that are not simple eutectic, but include binary phases,[13] and show a liquidus surface that varies continuously with the Ag/Au ratio.[13] We find that these alloys can therefore be used for both VSS and VLS growth. Alloying has already been used to design the $AlAu_2$ catalysts that have proven successful for VSS growth,[10] but the greater oxidation resistance of Ag, and the continuous range of alloy compositions available, make AgAu alloys more convenient and potentially more suitable for scale-up to standard chemical vapor deposition (CVD) growth conditions. We will demonstrate the growth of abrupt Si/Ge heterojunctions and the optimization of growth rates by controlling catalyst state, and we will also show the stability of these catalysts under appropriate growth conditions. We believe that the stability and properties of AgAu catalysts potentially open a promising route, *via* conventional chemical vapor deposition, toward control of group IV heterostructure nanowires.

RESULTS AND DISCUSSION

Nanowire Nucleation and Growth Using AgAu Catalysts. In Figure 1 we show the feasibility of Si nanowire growth from AgAu catalysts. The nanowires were grown *in situ* in a transmission electron microscope, enabling direct observation of the state of the catalyst, the structure of both catalyst and nanowire, and the growth kinetics of the nanowires. Details of the experiments are provided in the Methods section. Figure 1 illustrates nanowire growth from two different average catalyst compositions, $AgAu_2$ and Ag_2Au, with growth parameters, specifically the growth temperature, chosen on the basis of calculated pseudobinary phase diagrams.[13] It is clear that both VLS and VSS growth modes are possible, and we find that the mechanism depends on alloy composition and temperature. This is shown in Figure 1 panels a and d where VSS growth (from Ag_2Au and $AgAu_2$, respectively) is seen at temperatures below the lowest temperatures at which liquid is expected to be present on the calculated phase diagram, and Figure 1c where VLS growth (from $AgAu_2$) is seen above the calculated eutectic temperature. Note that

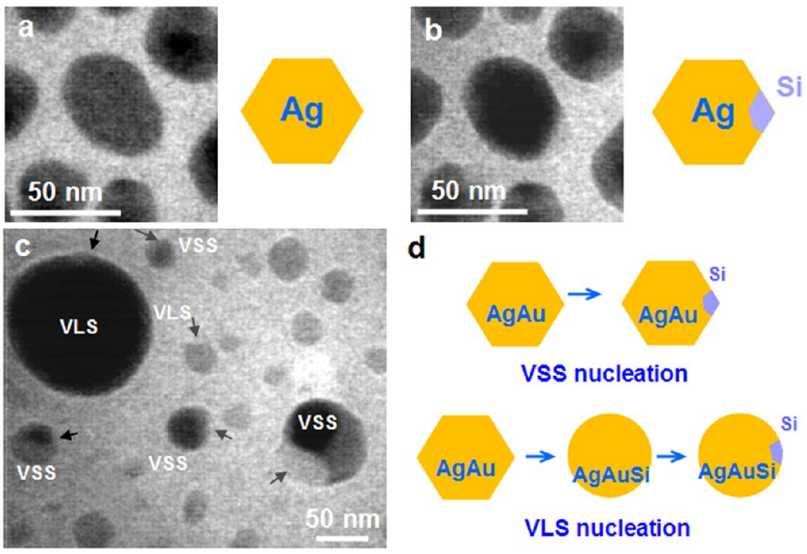

Figure 2. Nucleation of Si in the VSS and VLS modes. (a–b) VSS nucleation of Si from Ag particles. (a) Ag at 4 nm was deposited (without intentional heating) onto an electron transparent SiN membrane and was then heated to 490 °C to agglomerate into 20–50 nm faceted, polycrystalline particles. The image was obtained after heating to 550 °C and exposing to 1×10^{-5} Torr disilane. The particles remain solid, as indicated by their inhomogeneous contrast and their faceting. Note that faceting is not as clear as in Figure 1b because the substrate is amorphous and the particles do not show epitaxy. (b) The same area 6.5 s later, after nucleation has occurred at the arrowed location. Movie 1 shows dark field imaging of this particle during the time between images a and b. (c–d) VSS and VLS nucleation of Si from AgAu particles. Au aerosol particles followed by a 4 nm Ag film were deposited onto a SiN membrane and agglomerated, before heating to 580 °C and exposing to 5×10^{-6} Torr disilane. VSS and VLS processes, shown schematically, are visible in particles of presumably different Ag/Au ratios. The growth temperature corresponds to the eutectic temperature of Si with an alloy of composition Ag_2Au_3.

different nanowires show the same growth mode at a given temperature, VLS or VSS, suggesting that all catalyst particles in a given experiment have similar Ag/Au ratios.[19] Also, there is no apparent dependence of growth mode on the pressure of the precursor gas, disilane, over the narrow range of diameters and pressures that we examined.

VSS growth from AgAu alloys, as in Figure 1a,b,d, has some features in common with growth from other VSS catalysts, particularly $AlAu_2$. Viewed from above, the catalysts appear hexagonal, and the nanowires grow consistently (over 75%) in the [111] direction, with a corresponding hexagonal cross section with {211} sidewalls. VLS growth from AgAu alloys, Figure 1c, is similar in appearance to VLS growth from pure Au, also showing a hexagonal cross section with {211} sidewalls with "sawtooth"[20] faceting (seen more clearly in Figure 4). AgAu alloys in both VLS and VSS modes can thus produce nanowires of well-defined structure. AgAu alloys therefore appear promising as nanowire catalysts, although at the pressures available in our UHV–CVD system the growth rates are slow, especially for VSS, and higher pressure growth conditions may be required to form long nanowires.

Both VLS and VSS modes can be observed right from the start of nanowire growth. This is potentially important in circumstances where the structure at the base of a nanowire must be controlled. For example, the initial stages of growth of a nanowire *via* the VLS mode involve incorporation of material from the substrate (as well as from the gas phase) into the metal nanoparticle to form the eutectic liquid.[21] Nanowire growth *via* the VSS mode does not involve much initial incorporation of substrate material into the catalyst, due to the low solubility of the catalyst for the growth species.[7] Intermixing between substrate material and nanowire material should thus be reduced, making VSS growth preferable (in theory) if a heterojunction has to be formed at the base of the nanowire.

In Figure 2, we illustrate the two nucleation processes, VSS and VLS, with schematics of the stages of the reaction. Figure 2 panels a and b shows a VSS nucleation event for pure Ag, while Figure 2c shows both VSS and VLS processes, using a special sample described below in which alloy particles were prepared with a range of Ag/Au ratios.

VLS nucleation is commonly seen for Au above the eutectic temperature.[21–23] Here, dissociation of disilane and incorporation of Si leads first to formation of the AuSi eutectic, and then to the precipitation of a solid nucleus of Si from the liquid AuSi.[22–24] If the process takes place somewhat below the eutectic temperature, a supercooled liquid eutectic may still form and hence the VLS mode may still apply.[25,26] However, at sufficiently low temperatures, as for the Ag at 550 °C in Figure 2b, the particles appear to remain solid, with nucleation occurring heterogeneously at the edge of each particle. In Figure 2a,b, the solid nature of the particles can be deduced from their inhomogeneous contrast in bright-field imaging;

however, dark-field imaging (see Supporting Information video) shows the crystallinity of the particles in a more direct way and confirms that the Ag remains solid before and during the nucleation of Si under these conditions. Thus, a VSS process can be seen for pure Ag at sufficiently low temperature. We also see VSS nucleation for *alloy* particles, provided the temperature is sufficiently low. In Figure 2c, a sample was prepared in which each particle had a different Ag/Au ratio: first Au aerosol particles were deposited, then a uniform Ag film was added and the resulting alloy film was agglomerated. When heated with disilane, Figure 2c, some particles show VLS nucleation while others show VSS. Since we do not expect a strong effect of particle size on the nucleation process,[24] this difference in growth mode is presumably due to the variations in composition. The growth temperature may be above the eutectic temperature for particles that are Au-rich, resulting in VLS growth, but sufficiently far below for Ag-rich particles to result in VSS growth.

It is clear from this discussion that the control of particle composition is critical if we are to control the nucleation and growth modes of the nanowires. It is interesting to note that when an ensemble of particles is produced by annealing together two species with different surface mobilities, the coarsening process itself can lead to variations in composition between particles of different size.[27] For complete control of composition at the level of individual catalyst particles, it would therefore be worthwhile to start with size-selected core−shell AgAu particles.[28]

Growth Kinetics of Si Nanowires Formed Using AgAu Catalysts. To grow long nanowires, yet have the precision to form Si/Ge heterojunctions at specific locations, it is highly useful to be able to switch between the VLS and VSS growth modes.[10] In Figure 1d, VLS-grown Si nanowires were cooled during growth so that subsequent growth could continue by VSS. We now discuss the effect of this type of growth mode change on the growth kinetics, and the hysteresis in behavior when switching between high and low temperatures.

Figure 3a shows growth rates for three Si nanowires from the same sample, as the temperature is cycled to switch between VLS and VSS modes. Catalyst solidification and melting show hysteresis, as expected for a nanoscale system.[11] The hysteresis is broad, in this case occurring over a temperature range of approximately 60 °C. For each individual nanowire, the hysteretic switching between VLS and VSS can be repeated several times and allows growth of long nanowire sections by VLS, followed by slow and precise VSS growth that we will show below creates good heterostructures.

For VSS and VLS modes separately, it is clear from Figure 3a that growth rates increase with temperature. The temperature variation of growth rate is consistent with an Arrhenius dependence. The activation energies for VLS and VSS are similar, 0.25 ± 0.04 eV/atom and

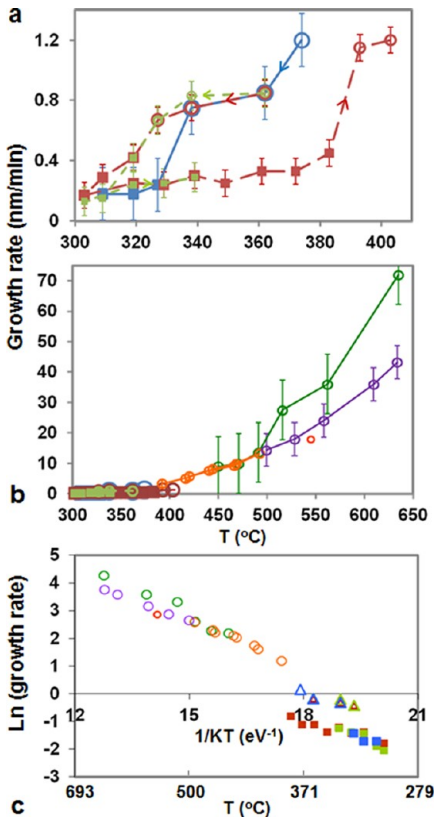

Figure 3. Kinetics of nanowires grown from Ag−Au catalysts. (a) Growth rates measured from three individual nanowires catalyzed by nominally $AgAu_2$ at 1×10^{-5} Torr disilane, shown in three different colors, with open circles indicating VLS and solid squares indicating VSS growth. The temperature was changed in the direction shown.[31] Three data points were obtained at each temperature by measuring the length of a nanowire every few minutes, then calculating the growth rate over each interval. (b, c) Linear and Arrhenius plots comparing growth rates of $AgAu_2$ catalyzed nanowires with Au catalyzed nanowires. The green and orange open circles indicate two separate sets of measurements made during growth of VLS Au catalyzed nanowires. The purple open circles are data for VLS Au catalyzed nanowires taken from ref 25. The VSS and VLS $AgAu_2$ data from panel a appears at the lower left of panel b and lower right of panel c. The red open circle indicates a higher temperature measurement from a separate VLS $AgAu_2$ growth. All data was obtained at 1×10^{-5} Torr disilane, apart from the green and purple symbols, for which the growth rates were normalized to the same pressure.

0.28 ± 0.06 eV/atom, respectively (Figure 3c). Over the (relatively small) temperature window where both VSS and VLS can be obtained, VLS growth rates are 3−4 times faster than VSS. Since the activation energies are the same within errors, we attribute this to changes in sticking coefficient;[12] the idea that the liquid surface provides an easier environment for adsorption of CVD gases compared to the flat, crystalline surface was first suggested in ref 5.

In Figure 3 panels b and c we compare growth rates from AgAu catalysts with data obtained from pure Au from three separate experiments. Note that temperature calibration is not straightforward for *in situ* TEM. Comparisons at a particular temperature between different samples, as

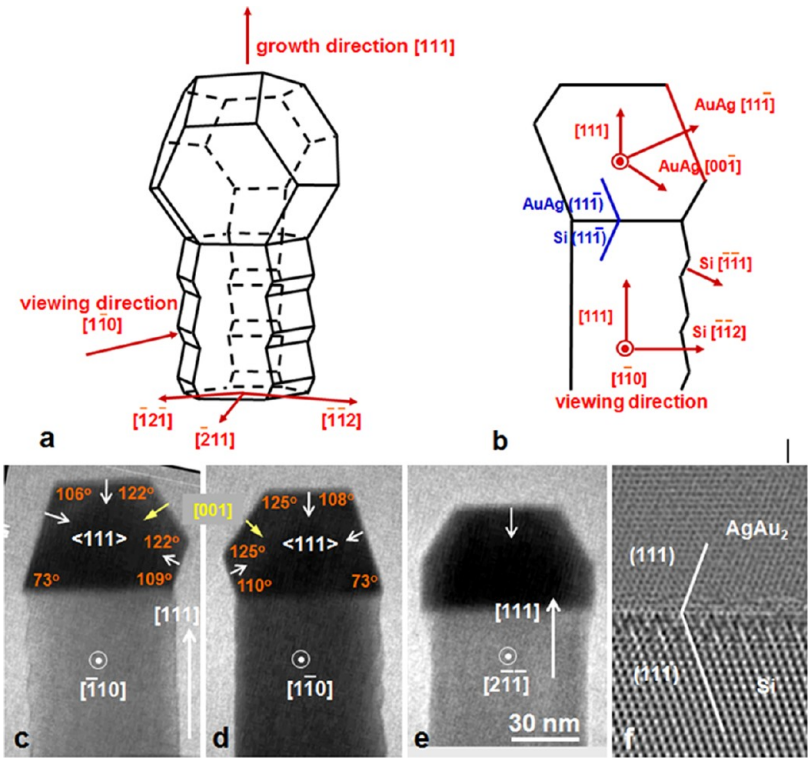

Figure 4. (a) A schematic diagram showing the orientation of the AgAu truncated octahadron on the sawtooth faceted Si nanowire. Although the diagram shows a regular truncated octahedron on a hexagonal nanowire, the nanowire cross section experimentally is a trigonal hexagon and the relative sizes of the AgAu {111} and {001} faces vary; some {001} faces may be absent, and the {111} faces are therefore not regular hexagons. (b) Projection of a in the [1$\bar{1}$0] viewing direction. The twin orientation is indicated. (c,d) Si nanowires grown from $AgAu_2$ by VLS followed by VSS, viewed in the [$\bar{1}$10] and [1$\bar{1}$0] directions. The two nanowires grow from the same substrate yet exhibit mirror symmetry, presumably due to a twin lower down on one wire. Sawtooth faceting is visible on one of the {211} sidewalls of each nanowire, confirming the twin relationship.[20] (e) Si nanowire grown from $AgAu_2$ by VLS then VSS, viewed in the ⟨211⟩ direction. (The vertical boundaries visible in the catalyst correspond to the projections of inclined edges of the truncated octahedron, and do not imply that {110} facets are present.) (f) Postgrowth high resolution C_s-corrected image of $AgAu_2$ on VSS-grown Si. The Si/$AgAu_2$ interface shows the B-type orientation relation.

is done here, can lead to errors that are higher than those expected if we compare nanowire growth at varying temperature on one sample, in which it is more likely that the entire temperature scale is offset but the trends in behavior with temperature are less likely to be distorted. With this caveat, a direct comparison of measurements at higher temperatures suggests similar rates for Au and AgAu (within a factor of 2), while extrapolation of the Au data to lower temperatures also yields growth rates similar to those in Figure 3a for VLS AgAu. Thus, AgAu catalyzes VLS growth at a rate that is not dramatically different from pure Au. However, the activation energy for AgAu is somewhat lower than the values obtained from the Au data at higher temperatures: 0.53 ± 0.02 eV/atom for the purple data taken from ref 29, 0.53 ± 0.01 eV/atom for the orange data, and 0.67 ± 0.02 eV/atom for the green data. It is encouraging for the development of alloy catalysts that the catalytic properties of Au are not decreased substantially by alloying with Ag; this conclusion is consistent with other studies that have used AgAu alloy catalysts.[30]

Reproducibility and Stability of Catalyst Structure. A key prerequisite for controlled nanowire growth from solid catalysts is a consistent catalyst shape and orientation

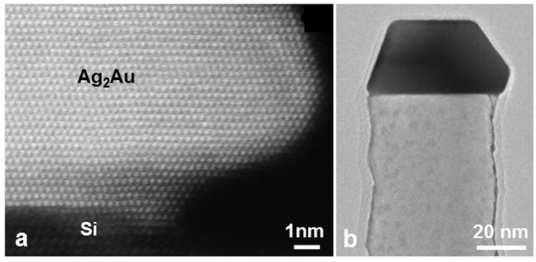

Figure 5. (a) Postgrowth high resolution C_s-corrected STEM image of Ag_2Au on VSS-grown Si, showing the crystallinity of the catalyst after several days of air exposure. (b) Postgrowth TEM image of an $AgAu_2$ catalyzed nanowire showing formation of a 1−2 nm amorphous surface layer on the catalyst (2−3 nm on the nanowire) after several days of air exposure. After removal from the UHV growth environment, nanowires were thinned by embedding in glue, mechanical polishing, and ion milling (for panel a) or were directly imaged with no additional preparation (for panel b).

relation, since the nanowire morphology and growth rate may depend on these details.[20] Ag and Au are face centered cubic with similar lattice parameters (within 0.2%). AgAu alloys share this structure, and AgAu nanoparticles may be expected to share the lowest energy facets of Au and Ag, the {111} and

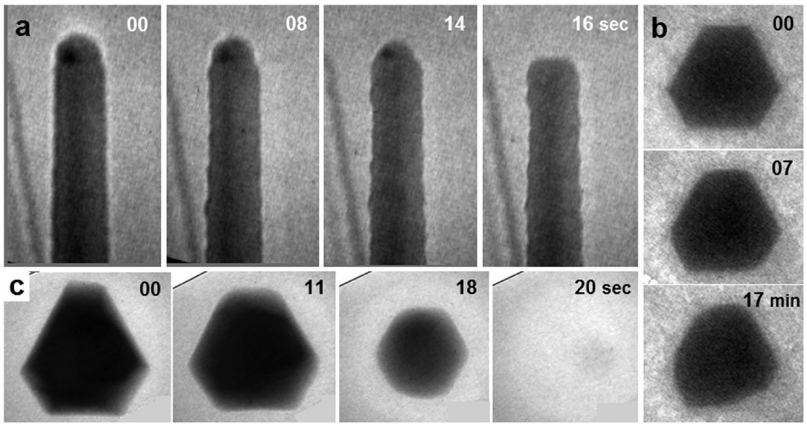

Figure 6. The stability of Ag−Au catalysts. (a) A Si nanowire imaged 2 min after the disilane flux was turned off, following 45 min of stable VSS growth with Ag_2Au at 550 °C and 5 × 10^{-6} Torr disilane, and the same nanowire after additional time indicated in seconds. The catalyst diffuses away from the tip within 16 s. (b) A solid faceted Ag_2Au catalyst atop a Si nanowire during growth at 540 °C and 1 × 10^{-5} Torr disilane, showing shape changes and loss of faceting at the times indicated in minutes since the disilane flux was switched off. (c) An Ag particle on a planar Si(111) surface showing diffusion at 480 °C. The time elapsed in seconds is indicated. This can be compared with nanowire growth from pure Ag (not shown), in which Ag remains stable at 620 °C and 1 × 10^{-5} Torr disilane over tens of minutes allowing VSS Si nanowire growth at 0.4 nm min^{-1}.

{001} surfaces.[32,33] We find that, unlike say the VSS catalyst Cu_3Si,[34] AgAu catalysts display consistent faceting and orientation relations with their nanowires over the window of alloy composition, growth temperature, and gas pressure that we have examined.

The details of the catalyst shape and orientation relation are shown in Figure 4a,b. The projection of the catalysts as seen during growth, Figure 4c−e, is consistent with {111} and {001} bounding facets, that is, a truncated octahedral shape. However, the catalysts are not regular truncated octahedra; in particular the {001} facet adjacent to the nanowire is often small or absent, and higher index facets can be present (as in Figure 7b, lower left corner). We find that these truncated octahedra are oriented on the Si nanowire with an AgAu ⟨111⟩ direction parallel to the Si [111] nanowire growth direction, but rotated so that there is a twin relationship between the lattices. This rotated orientation can be demonstrated from the position of the sawtooth faceting on one of the two sidewalls that are visible for each nanowire. Sawtooth faceting is clearly visible on only three of the six sidewalls (at least, for nanowire growth from pure Au[20]), as shown in Figure 4a, and its position therefore allows the Si orientation to be determined unambiguously. From Figure 1d, we find that irregular truncated octahedra can be present on over 80% of the nanowires. The high symmetry of the catalyst crystal structure (compared to say Cu_3Si[34] or $AlAu_2$[11]) may be related to this reproducibility.

Postgrowth aberration corrected TEM imaging of VSS-grown nanowires (Figure 4f) directly demonstrates that the catalyst facets are made up of {111} and {001} planes, and also shows that AgAu and Si have the twinned, or "B-type" orientation relation expected from the discussion above. The interface actually contains a high density of dislocations (one every 0.95 nm), since the measured lattice mismatch between $AgAu_2$ and Si is 25%.

We can assess the environmental stability of the catalysts from the postgrowth high resolution images. Figure 5 shows that there is no strong oxidation reaction, with only a thin amorphous layer formed on the catalyst (slightly thicker on the nanowire surface). No amorphization of the metal particle is visible. This is in contrast to the strongly oxidizing case of $AlAu_2$,[11] confirming the expected resistance of AgAu alloys to oxidation when exposed to a non-UHV environment.

As well as environmental stability, it is also important that a nanowire catalyst be stable at the nanowire tip during growth, and not change its volume, say by diffusion of catalyst atoms.[35] The importance of this requirement can be appreciated by considering that for Si nanowires grown from Au, surface diffusion and coarsening of Au can change the catalyst volume, create tapered nanowires and limit the achievable nanowire length, especially for higher temperatures and lower growth rates.[35] The possibility of surface diffusion of Au and Ag, particularly given the higher temperatures required for VLS growth with AgAu compared to pure Au, mean that overcoming catalyst instability is key to controlled growth. Conveniently, we find that the growth environment itself, specifically the presence of disilane, appears to stabilize the catalysts. We find that AgAu particles can maintain stable shapes and sizes over tens of minutes during growth, but when the flux is switched off their shapes and volumes can change dramatically (Figure 6a,b). Pure Ag shows similar effects (Figure 6c), suggesting that Ag is mobile as well as Au. For Au, surface diffusion on Si is known to be suppressed at high disilane pressures;[36] we speculate that a similar phenomenon may work for Ag. Accordingly, maintaining a flow of source gas appears to be important in achieving stable growth.[37]

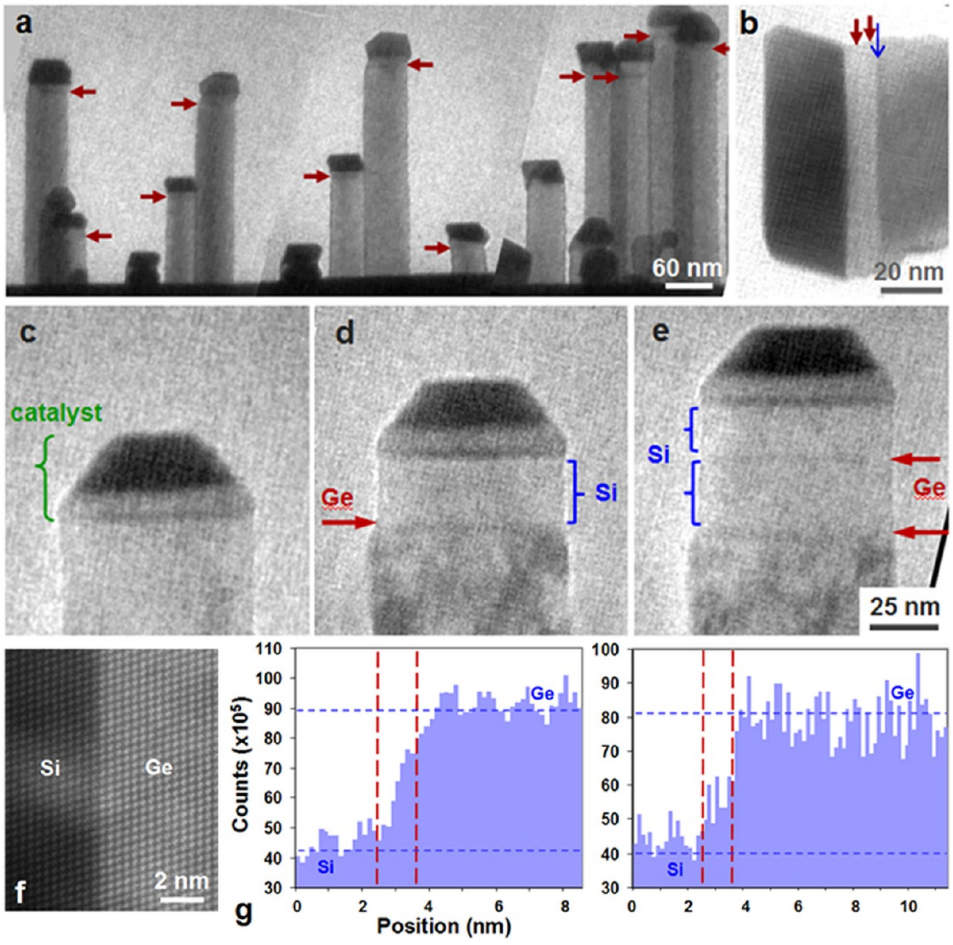

Figure 7. Si/Ge/Si heterostructures. (a) Low magnification image of Si nanowires with each Ge layer arrowed. VSS Si growth was at 415 °C and 5 × 10^{-6} Torr disilane and Ge at 366 °C and 1 × 10^{-6} Torr digermane. (b) A single nanowire with two Ge thin layers (~1.1 nm-thick) indicated with red arrows. VSS Si growth was at 360 °C and 5 × 10^{-6} Torr disilane and Ge at 330 °C and 1 × 10^{-6} Torr digermane. The contrast change indicated by the blue arrow is due to a twin in the Si that occurred at the switch from VLS to VSS Si growth. (c) A Si nanowire grown from $AgAu_2$ by VLS at 510 °C and 1 × 10^{-5} Torr disilane then by VSS at 383 °C. The contrast change in the catalyst is due to a twin. (d) The same nanowire after VSS growth of a Si/Ge/Si heterojunction. Ge was grown at 340 °C and 5 × 10^{-6} Torr digermane followed by Si at 393 °C and 1 × 10^{-5} Torr disilane. Conformal Ge growth on the nanowire sidewall is visible as mottled contrast. (e) The same nanowire now with a Si/Ge/Si/Ge/Si heterojunction. The second Ge layer was grown at 310 °C and 5 × 10^{-6} Torr digermane and Si at 383 °C and 1 × 10^{-5} Torr disilane. At this lower Ge growth temperature, conformal Ge is much less evident. (f) High resolution HAADF STEM image of a VSS Si/Ge interface with a thick Ge segment. (g) Line profiles across the Si/Ge interface in two nanowires both grown as follows: VLS $AgAu_2$ at 482 °C and 5 × 10^{-6} Torr disilane, followed by VSS growth at 360 °C; VSS Ge growth at 330 °C and 1 × 10^{-6} digermane, then VSS Si at 360 °C and 5 × 10^{-6} Torr disilane. The width of the compositional change (20%−80%) is indicated and is 1.2 ± 0.01 nm, of which 0.7 nm can be attributed to beam broadening and multiple scattering.

The Formation of Compositionally Abrupt Si/Ge Interfaces. In Figure 7 we use AgAu catalysts, with their ability to switch between VSS and VLS modes, their consistent crystal structures and orientation relation, and their environmental stability, to direct the fabrication of Si/Ge/Si heterojunctions with a reasonable yield. A long segment of Si is grown by VLS, and then a rapid reduction in temperature transforms the growth to the VSS mode. The gas supply is switched from Si to Ge at the low temperature, and a narrow Ge layer is grown. Finally, another VSS Si segment is grown to encapsulate the Ge segment (Figure 7a). During the cycling of temperature and gas species we did not observe changes in the catalyst shapes. (Changing the gas species at higher temperatures can result in a catalyst shape change, so was avoided.) The structures formed do not appear to show defects such as interfacial dislocations, and are therefore coherently strained.[38]

This process can be repeated to produce multiple Ge layers (Figure 7b). During Ge growth, a low temperature is preferable for avoiding conformal deposition. This is illustrated in Figure 7c−e, where the two Ge layers were formed at two different temperatures. Growth of the first Ge layer, at a higher temperature, results in collateral deposition of Ge on the surface of the nanowire. The second Ge layer, formed at lower temperature, is not associated with visible conformal Ge deposition.

To evaluate the compositional abruptness of the Si/Ge interfaces, we performed postgrowth measurement of composition along the nanowire growth direction using

high angle annular dark-field STEM. Line scans along nanowires show a measured compositional abruptness (evaluated from the 20−80% contrast change) of l.2 ± 0.1 nm across the VSS grown Si/Ge interfaces (Figure 7f). Accounting for the effects of multiple scattering and beam broadening[10] suggests a true compositional abruptness of 1.3 nm. Ge quantum wells with abrupt interfaces are expected to show high strain fields and therefore strong carrier confinement effects, and are therefore of great interest in electronic device design.[39] Useful nanowire lengths for device studies could be achieved by continuing the growth of Si by VSS or VLS after forming the heterojunction. In practical terms, a growth pressure that is higher than we can attain in the UHV-TEM would be helpful for achieving this.

CONCLUSIONS

We have demonstrated the use of a new AgAu alloy catalyst for the formation of nanowires and Si/Ge/Si heterojunctions with compositionally abrupt interfaces. AgAu alloy catalysts provide excellent flexibility in controlling a key parameter, the eutectic temperature, and therefore afford us the ability to switch between VLS and VSS growth modes. We have shown that these catalysts also satisfy stability and reproducibility requirements. Solid AgAu catalysts display a consistent faceting and orientation on the nanowire tips. The catalyst structure and lattice parameter do not depend strongly on composition, unlike the case for AlAu alloys. They are relatively insensitive to the environment, compared to Al-based catalysts, and are stable to diffusion during growth providing gas flow is maintained.

We believe that alloy catalysts in general open up a promising route toward control of nanowire and heterostructure growth and morphology, and Ag−Au in particular is an attractive materials system for structural control in Si/Ge nanowires.

METHODS

The nanowire growth experiments took place *in situ* in a Hitachi H-9000 UHV transmission electron microscope (TEM) with a base pressure of 2×10^{-10} Torr and a maximum gas pressure during observation of 1×10^{-5} Torr. For examination of growth kinetics, the substrate used was a chemically cleaned Si(111) wafer that was mounted in the TEM so that the electron beam was parallel to the surface. The wafers were cut so that the electron beam was parallel to either a ⟨110⟩ or a ⟨211⟩ direction. Plan-view observations were also made, using samples with a Si (111) or SiN membrane. For each type of sample, a chemical clean was performed before loading into the UHV system, and flash cleaning was then carried out *ex situ* in an adjacent UHV chamber at 1250 °C to desorb surface oxide. Au and Ag were then sequentially deposited at a pressure below 5×10^{-9} Torr. Each deposition rate was measured using a conventional crystal monitor (*via* the change of resonant frequency due to deposited mass). This enabled the average Ag/Au ratio to be measured, and this average is the value cited in the text. A total thickness of ∼4 nm of Ag plus Au was used. The substrate was transferred under UHV to the microscope and resistively heated to the growth temperature. This enabled agglomeration of the film into particles. The reaction gases for Si and Ge growth, disilane and digermane, respectively, were leaked into the TEM polepiece area through a capillary tube to a partial pressure in the range 5×10^{-6} to 1×10^{-5} Torr. The sample temperature was calibrated pre- and postgrowth using an infrared pyrometer. Images were recorded at 30 frames per second onto video tape and subsequently digitized for analysis of growth kinetics. Aberration- (C_s-) corrected high resolution phase-contrast images were obtained postgrowth using an FEI Titan 80−300 transmission electron microscope. Measurements of compositional abruptness in Si/Ge heterostructures were also obtained postgrowth, using high angle annular dark field imaging in a C_s-corrected Hitachi HD2700C scanning transmission electron microscope.

Conflict of Interest: The authors declare no competing financial interest.

Acknowledgment. The authors acknowledge financial assistance from the NSF under Grant No. DMR-0907483. Research was carried out in part at the Center for Functional Nanomaterials, Brookhaven National Laboratory, which is supported by the U.S. Department of Energy, Office of Basic Energy Sciences, under Contract No. DE-AC02-98CH10886.

Supporting Information Available: A TEM video recorded using dark-field imaging conditions, showing nucleation of Si from the Ag particle shown in Figure 2a,b. The particle is approximately 45 nm in diameter in a 115 nm × 115 nm field of view. Nucleation took place on a SiN substrate at 550 °C and 1×10^{-5} Torr disilane. A dark-field image is formed from electrons that were diffracted by a particular set of crystal planes. Thus, wherever the image is bright, the Ag particle is crystalline *and* one set of planes is at the correct angle to the beam for strong diffraction. Initially, the Ag shows uniform bright contrast, suggesting it is single crystal. Si nucleates after about 2 s; it is not clearly visible because its lattice planes are not oriented correctly, but its position can be seen in Figure 2b. At this moment the particle brightness decreases abruptly, but does not go to zero. We interpret this as the Ag remaining crystalline but slightly rotated; in other words, a VSS nucleation process. This material is available free of charge *via* the Internet at http://pubs.acs.org.

Note Added after ASAP Publication: After this article was published ASAP on July 2, 2012, the author list for ref 10 was corrected. The paper was reposted July 11, 2012.

REFERENCES AND NOTES

1. Gudiksen, M. S.; Lauhon, L. J.; Wang, J.; Smith, D. C.; Lieber, C. M. Growth of Nanowire Superlattice Structures for Nanoscale Photonics and Electronics. *Nature* **2002**, *415*, 617–620.
2. Yang, C.; Zhong, Z.; Lieber, C. M. Encoding Electronic Properties by Synthesis of Axial Modulation-Doped Silicon Nanowires. *Science* **2005**, *310*, 1304–1307.
3. Björk, M. T.; Thelander, C.; Hansen, A. E.; Jensen, L. E.; Larsson, M. W.; Wallenberg, L. R.; Samuelson, L. Few-Electron Quantum Qots in Nanowires. *Nano Lett.* **2004**, *4*, 1621–1625.
4. Li, D.; Wu, Y.; Fan, R.; Yang, P.; Majumdar, A. Thermal Conductivity of Si/SiGe Superlattice Nanowires. *Appl. Phys. Lett.* **2003**, *83*, 3186–3188.
5. Wagner, R. S.; Ellis, W. C. Vapor−Liquid−Solid Mechanism of Single Crystal Growth. *Appl. Phys. Lett.* **1964**, *4*, 89–90.
6. Wagner, R. S., VLS Mechanism of VLS Growth. In *Whisker Technology*; Levitt, A. P., Ed.; Willey Interscience: New York, 1970; p 47.
7. Li, N.; Tan, T. Y.; Gösele, U. Transition Region Width of Nanowire Hetero- and pn-Junctions Grown Using Vapor−Liquid−Solid Processes. *Appl. Phys. A: Mater. Sci. Process.* **2008**, *90*, 591–596.

8. Clark, T. E.; Nimmatoori, P.; Lew, K. -K.; Pan, L.; Redwing, J. M.; Dickey, E. C. Diameter Dependent Growth Rate and Interfacial Abruptness in Vapor−Liquid−Solid $Si/Si_{1-x}Ge_x$ Heterostructure Nanowires. *Nano Lett.* **2008**, *8*, 1246–1252.
9. Perea, D. E.; Li, N.; Dickerson, R. M.; Misra, A.; Picraux, S. T. Controlling Heterojunction Abruptness in VLS-grown Semiconductor Nanowires *via in Situ* Catalyst Alloying. *Nano Lett.* **2011**, *11*, 3117–3122.
10. Ben-Ishai, M.; Patolsky, F. From Crystalline Germanium−Silicon Axial Heterostructures to Silicon Nanowire−Nanotubes. *Nano Lett.* **2012**, *12*, 1121–1128.
11. Wen, C.-Y.; Reuter, M. C.; Bruley, J.; Tersoff, J.; Kodambaka, S.; Stach, E. A.; Ross, F. M. Formation of Compositionally Abrupt Axial Heterojunctions in Silicon−Germanium Nanowires. *Science* **2009**, *326*, 1247–1250.
12. Schmidt, V.; Wittemann, J. V.; Gösele, U. Growth, Thermodynamics, and Electrical Properties of Silicon Nanowires. *Chem. Rev.* **2010**, *110*, 361–388.
13. Prince, A. Silver−Gold−Silicon. In *Thermodynamic Properties, Ternary Alloy Systems: Phase Diagrams, Crystallographic and Thermodynamic Data Critically Evaluated by MSIT*; Springer-Verlag: New York, 2006 (updated by Fabrichnaya, O.).
14. Wang, Y.; Schmidt, V.; Senz, S.; Gösele, U. Epitaxial Growth of Silicon Nanowires Using an Aluminium Catalyst. *Nat. Nanotechnol.* **2006**, *1*, 186–189.
15. Wacaser, B. A.; Reuter, M. C.; Khayyat, M. M.; Wen, C.-Y.; Haight, R.; Guha, S.; Ross, F. M. Growth System, Structure, and Doping of Aluminum-Seeded Epitaxial Silicon Nanowires. *Nano Lett.* **2009**, *9*, 3296–3301.
16. Nebol'sin, V. A.; Shchetinin, A. A.; Dolgachev, A. A.; Korneeva, V. V. Effect of the Nature of the Metal Solvent on the Vapor−Liquid−Solid Growth Rate of Silicon Whiskers. *Inorg. Mater.* **2005**, *41*, 1256–1259.
17. Wagner, R. S.; Ellis, W. C. Vapor−Liquid−Solid Mechanism of Crystal Growth and its Application to Silicon. *Trans. Met. Soc. AIME* **1965**, *233*, 1053–1064.
18. Wittemann, J. V.; Münchgesang, W.; Senz, S.; Schmidt, V. Silver Catalyzed Ultrathin Silicon Nanowires Grown by Low-Temperature Chemical-Vapor-Deposition. *J. Appl. Phys.* **2010**, *107*, 096105.
19. We cannot measure the composition of individual particles directly. However (except for the special case of Figure 2c), particles show similar solidification and melting temperatures—each particle in the field of view solidifies as the temperature is reduced through a 10−15 °C window, say—and the temperatures do not change if we repeatedly heat and cool the sample. Since changes in Ag/Au ratio would change the eutectic temperature, we do not believe that there are large differences in Ag/Au ratio between particles, or that the ratio changes with time for an individual particle.
20. Ross, F. M.; Tersoff, J.; Reuter, M. C. Sawtooth Faceting in Silicon Nanowires. *Phys. Rev. Lett.* **2005**, *95*, 146104.
21. Wagner, R. S. Defects in Silicon Crystals Grown by the VLS Technique. *J. Appl. Phys.* **1967**, *38*, 1554.
22. Kim, B. J.; Tersoff, J.; Kodambaka, S.; Reuter, M. C.; Stach, E. A.; Ross, F. M. Kinetics of Individual Nucleation Events Observed in Nanoscale Vapor−Liquid−Solid Growth. *Science* **2008**, *322*, 1070–1073.
23. Hofmann, S.; Sharma, R.; Wirth, C. T.; Cervantes-Sodi, F.; Ducati, C.; Kasama, T.; Dunin-Borkowski, R. E.; Drucker, J.; Bennett, P.; Robertson, J. Ledge-Flow-Controlled Catalyst Interface Dynamics during Si Nanowire Growth. *Nat. Mater.* **2008**, *7*, 372–375.
24. Kim, B. J.; Tersoff, J.; Wen, C. Y.; Reuter, M. C.; Stach, E. A.; Ross, F. M. Determination of Size Effects during the Phase Transition of a Nanoscale Au−Si Eutectic. *Phys. Rev. Lett.* **2009**, *103*, 155701.
25. Gamalski, A. D.; Tersoff, J.; Sharma, R.; Ducati, C.; Hofmann, S. Formation of Metastable Liquid Catalyst during Subeutectic Growth of Germanium Nanowires. *Nano Lett.* **2010**, *10*, 2972–2976.
26. Kodambaka, S.; Tersoff, J.; Ross, F. M. Ge Nanowire Growth below the Eutectic Temperature. *Science* **2007**, *316*, 729–732.
27. Alloyeau, D.; Prévot, G.; Le Bouar, Y.; Oikawa, T.; Langlois, C.; Loiseau, A.; Ricolleau, C. Ostwald Ripening in Nanoalloys: When Thermodynamics Drives a Size-Dependent Particle Composition. *Phys. Rev. Lett.* **2010**, *105*, 255901.
28. Wu, Y.; Jiang, P.; Jiang, M.; Wang, T. W.; Guo, C. F.; Xie, S. S.; Wang, Z. L. The Shape Evolution of Gold Seeds and Gold@Silver Core−Shell Nanostructures. *Nanotechnology* **2009**, *20*, 305602.
29. Kodambaka, S.; Tersoff, J.; Reuter, M. C.; Ross, F. M. Diameter-Independent Kinetics in the Vapor−Liquid−Solid Growth of Si Nanowires. *Phys. Rev. Lett.* **2006**, *96*, 096105.
30. Sandoval, A.; Aguilar, A.; Louis, C.; Traverse, A.; Zanella, R. Bimetallic Au-Ag/TiO_2 Catalyst Prepared by Deposition-Precipitation: High Activity and Stability in CO Oxidation. *J. Catal.* **2011**, *281*, 40–49.
31. The melting temperature observed, 390 °C, is lower than the expected eutectic temperature for $AgAu_2$ of 536 °C. We believe this is due to an error in temperature calibration for this data set, which was calibrated by measuring current through the sample (all other experiments were calibrated by measuring power dissipated in the sample).
32. Wang, Z.; Wynblatt, P. The Equilibrium Form of Pure Gold Crystals. *Surf. Sci.* **1998**, *398*, 259–266.
33. Wiley, B.; Sun, Y.; Xia, Y. Synthesis of Silver Nanostructures with Controlled Shapes and Properties. *Acc. Chem. Res.* **2007**, *40*, 1067–1076.
34. Wen, C.-Y.; Reuter, M. C.; Tersoff, J.; Stach, E. A.; Ross, F. M. Structure, Growth Kinetics, and Ledge Flow during Vapor−Solid−Solid Growth of Copper-Catalyzed Silicon Nanowires. *Nano Lett.* **2010**, *10*, 514–519.
35. Hannon, J. B.; Kodambaka, S.; Ross, F. M.; Tromp, R. M. The Influence of the Surface Migration of Gold on the Growth of Silicon Nanowires. *Nature* **2006**, *440*, 69–71.
36. Madras, P.; Dailey, E.; Drucker, J. Spreading of Liquid AuSi on Vapor−Liquid−Solid-Grown Si Nanowires. *Nano Lett.* **2010**, *10*, 1759–1763.
37. Dailey, E.; Madras, P.; Drucker, J. Au on Vapor−Liquid−Solid Grown Si Nanowires: Spreading of Liquid AuSi from the Catalytic Seed. *J. Appl. Phys.* **2010**, *108*, 064320.
38. Larsson, M. W.; Wagner, J. B.; Wallin, M.; Håkansson, P.; E Fröberg, L.; Samuelson, L.; Wallenberg, L. R. Strain Mapping in Free-Standing Heterostructured Wurtzite InAs/InP Nanowires. *Nanotechnology* **2007**, *18*, 015504.
39. Swadener, J. G.; Picraux, S. T. Strain Distributions and Electronic Property Modifications in Si/Ge Axial Nanowire Heterostructures. *J. Appl. Phys.* **2009**, *105*, 044310.